

Granular systems in the Coulomb blockade regime

D. P. Arovas¹, F. Guinea², C. P. Herrero², P. San José²

¹ *Department of Physics, University of California at San Diego, La Jolla CA 92093*

² *Instituto de Ciencia de Materiales de Madrid, CSIC, Cantoblanco, E-28049 Madrid, Spain.*

(Dated: February 1, 2008)

Disordered granular systems, at temperatures where charging effects are important, are studied, by means of an effective medium approximation. The intragrain charging energy leads to insulating behavior at low temperatures, with a well defined Coulomb gap. Non equilibrium effects can give rise to a zero temperature transition between a metallic, gapless phase, and an insulating phase.

I. INTRODUCTION

Charging effects modify the transport properties of granular metals at low temperatures^{1,2,3}. In magnetic systems, the low temperature magnetoresistance can also be modified by charging effects^{4,5,6,7,8,9}.

A successful scheme used to analyze Coulomb blockade in granular systems is to reduce the system to the study of an effective single junction, as in the pioneering study done in Ref. 10. This assumes that each junction has an activated conductance, which is approximately correct when the high temperature conductance of the junction g , is low in units of e^2/\hbar . A single junction in the Coulomb blockade regime has been extensively studied in recent years¹¹. Modern techniques allow us to study the behavior of a single junction for arbitrary values of the conductance and offset charges (see below).

The current approach describes a single junction in terms of two collective variables, the charge, Q , and its conjugate phase variable, ϕ . The electronic degrees of freedom are integrated out^{12,13}. This procedure is motivated by a similar approach used in the study of small Josephson junctions¹⁴. The present tools allow us to study junctions with high values of the conductance, $g \gg e^2/\hbar$, and to consider the effect of gate voltages, and of degeneracies between different charge states. The model can be extended to study non equilibrium processes associated to the tunneling events^{15,16}, which can be considered as the leading corrections in an expansion in g^{-1} , where g is the intragrain conductance^{17,18}.

In the following, we will extend these standard methods used in the study of Coulomb blockade in single junc-

tions to the analysis of granular materials. In order to do so, we will use an effective medium theory. This approach can be viewed as an extension to mesoscopic systems of the Dynamical Mean Field Theory used in the study of the microscopic properties of strongly correlated systems¹⁹. The model and method of calculation will be presented in the next section. Section III discusses results obtained using analytical large- N techniques which describe well the properties of single junctions^{20,21}. Then, we show numerical results obtained using Monte Carlo (MC) methods previously applied to the study of single junctions²². Section IV contains the main conclusions of our work.

II. THE MODEL

A. Effective medium theory.

We will consider a system made of metallic grains. We assume that the separation of the electronic states within each grain, δ_i , is much smaller than the charging energies, E_c^i , or the temperature, $k_B T$. The grains are connected by a large number of channels with small transmission coefficients, so that a perturbative treatment of the coupling induced by each individual channel is possible. Then, the electronic degrees of freedom can be integrated out^{12,13,14,23}, and the system is described in terms of the charge at each grain, Q_i , and its conjugated phase variable, ϕ_i , where $[Q_i, \phi_i] = ie$, and e is the unit of charge. The effective action which describes the charge effects in the system is, at zero temperature:

$$\mathcal{S} = \frac{1}{2e^2} \sum_{i,j} \int_0^\beta d\tau C_{ij} (\partial_\tau \phi_i) (\partial_\tau \phi_j) + \sum_{i < j} \alpha_{ij} \int_0^\beta d\tau \int_0^\beta d\tau' K(\tau - \tau') \left\{ 1 - \cos [\phi_i(\tau) - \phi_j(\tau) - \phi_i(\tau') + \phi_j(\tau')] \right\}, \quad (1)$$

where $K(\tau) = [\pi T \csc(\pi T \tau)]^2$ (we henceforth set $k_B \equiv 1$). We further assume that the capacitance matrix is dominated by its diagonal entries, and identify the charging energy of the i^{th} grain as $E_c^i = e^2/2C_{ii}$. The coupling be-

tween grains i and j is $\alpha_{ij} = 2|t_{ij}|^2 \rho_i \rho_j$, where t_{ij} is the hopping matrix element between the grains (assumed independent of momenta), and $\rho_{i,j}$ are the respective densities of states. One can also write $\alpha_{ij} = R_K/4\pi^2 R_{ij}$,

where $R_K = h/e^2 = 25,813 \Omega$ is the quantum of resistance and R_{ij} is the high-temperature value of the inter-grain resistance.

The above model possesses a global $O(2)$ rotational symmetry, which may be generalized to an $SU(N)$ sym-

metry as follows. On each site, we replace the unimodular complex scalar $z_i \equiv e^{i\phi_i}$ with an N -component unimodular complex vector with components $z_{i\mu}$ ($\mu = 1, \dots, N$). The action for the $SU(N)$ model is then

$$S = \sum_i \frac{1}{4E_c^i} \int_0^\beta d\tau (\partial_\tau z_{i\mu}^*) (\partial_\tau z_{i\mu}) + \sum_{i < j} \alpha_{ij} \int_0^\beta d\tau \int_0^\beta d\tau' K(\tau - \tau') \left\{ 1 - z_{i\mu}^*(\tau) z_{j\mu}(\tau) z_{i\nu}(\tau') z_{j\nu}^*(\tau') \right\} \quad (2)$$

We now assume that each grain is coupled to a large number, M , of other grains, and define the mean field correlation function $G_i(\tau - \tau')$ as

$$\frac{M}{N} G_i(\tau - \tau') \delta_{\mu\nu} \equiv \frac{1}{\bar{\alpha}} \left\langle \sum_j \alpha_{ij} z_{j\mu}(\tau) z_{j\nu}^*(\tau') \right\rangle, \quad (3)$$

with $\bar{\alpha} \equiv M^{-1} \langle \sum_j \alpha_{ij} \rangle$ the average coupling of a grain to its neighbors. Note that $G(0) = 1$. This allows us to write the action as a sum over contributions from individual grains, with the effective self-interaction term

$$S_i^{\text{int}} = \tilde{\alpha} \int_0^\beta d\tau \int_0^\beta d\tau' K(\tau - \tau') \left\{ 1 - G_i(\tau - \tau') z_{i\mu}^*(\tau) z_{i\mu}(\tau') \right\} \quad (4)$$

with $\tilde{\alpha} \equiv M\bar{\alpha}/N$. Thus, the properties of the system can be reduced to those of a single junction embedded in an effective environment whose properties are to be determined self consistently.

B. Offset charges and non equilibrium effects.

We can extend the model discussed so far to situations when there are offset charges, q_i , at each grain. These offset charges lead to additional phases in the contributions of paths of $\phi(\tau)$ with non zero winding numbers. A path of winding number m acquires a phase $\chi_i = 2\pi m q_i$. This phase has to be added to the effective action, Eq.(1).

The same scheme can also be used to include the effect of non equilibrium processes associated to intergrain tunneling^{15,16}. The electron which tunnels induces an inhomogeneous electrostatic potential, which modifies the

electronic levels within the grain. This effect can be analyzed using similar techniques to those used in relation to the sudden ejection of a core electron in a metal²⁴, and it leads to a modification of the kernel in the term which describes the tunneling in the action in Eq.(1). The decay of the interaction $K(\tau - \tau')$ at long times becomes $|\tau - \tau'|^{2-\epsilon}$, where ϵ is a dimensionless parameter, which can be expressed in terms of the phaseshifts induced at the Fermi level by the sudden switching of the external potential. A similar effect is expected if the tunneling takes place between quasi one-dimensional systems²⁵.

In fact, for each pair of grains one should replace the kernel $K(\tau)$ with

$$K_{ij}(\tau) = (E_c^i)^{\epsilon_i} (E_c^j)^{\epsilon_j} [\pi T \csc(\pi T \tau)]^{2-\epsilon_i-\epsilon_j}. \quad (5)$$

For the sake of simplicity, we will assume

$$K(\tau) = \overline{E_c}^\epsilon [\pi T \csc(\pi T \tau)]^{2-\epsilon} \quad (6)$$

for all pairs, where $\overline{E_c}$ is the average charging energy.

C. Monte Carlo procedure

In our effective-medium scheme, the grand partition function for a generic grain i with a given offset charge q_i can be written in terms of the phase ϕ_i , as²³:

$$Z(q_i) = \sum_{m=-\infty}^{\infty} \exp(i\chi_i) \int \mathcal{D}\phi_i \exp(-\mathcal{S}_{\text{eff}}[\phi_i]) \quad (7)$$

where the paths $\phi_i(\tau)$ satisfy in sector m the boundary condition $\phi_i(\beta) = \phi_i(0) + 2\pi m$. The effective action takes the form:

$$\mathcal{S}_{\text{eff}}[\phi] = \frac{1}{4\overline{E_c}} \int_0^\beta d\tau \left(\frac{\partial \phi}{\partial \tau} \right)^2 + \tilde{\alpha} \int_0^\beta d\tau \int_0^\beta d\tau' K(\tau - \tau') \{ 1 - \cos[\phi(\tau) - \phi(\tau')] G(\tau - \tau') \} \quad (8)$$

with the kernel $K(\tau)$ given in Eq. (6). It describes low-energy processes below an upper cutoff on the order of

the unscreened average charging energy, $\overline{E_c}$. Here, the

correlation function G is given by

$$G(\tau - \tau') = \langle \cos[\phi(\tau) - \phi(\tau')] \rangle, \quad (9)$$

where the average value is calculated with the partition function in Eq. (7). Note that the action in Eq. (8) is similar to that corresponding to a single tunnel junction with dimensionless conductance $\tilde{\alpha}$ and charging energy \overline{E}_c , the only difference being the presence of the correlator G in the tunneling part of the effective action of the granular system.

Different sectors (winding numbers m) in the partition function $Z(q_i)$ have been sampled by path-integral Monte Carlo for temperatures down to $T = \overline{E}_c/50$. MC simulations have been carried out by the usual discretization of quantum paths into N (Trotter number) imaginary-time slices²⁶. To keep roughly the same precision in the calculated quantities, as the temperature is reduced, the number of time slices has to be increased as $1/T$. We have taken $N = 4\beta\overline{E}_c$, and thus, we employed an imaginary-time slice $\Delta\tau = \beta/N = 1/(4\overline{E}_c)$. Details on this kind of MC simulations were given in earlier publications^{17,22} and will not be repeated here.

From a computational point of view, the main difference between the present procedure and that used in earlier works^{17,22} is the requirement of self-consistency for the correlator $G(\tau - \tau')$, as expressed by Eqs. (8) and (9). To obtain this self-consistency, we employed an iterative procedure that led to convergence of the correlator in the region of parameters studied here. For a given set of parameters (T , $\tilde{\alpha}$, ϵ , and q_i), we begin the simulations by assuming a correlator $G_0(\tau - \tau') = 1$. The correlator G_1 obtained by introducing G_0 in the effective action Eq.(8) is then employed in a new iteration to obtain G_2 , and so on. In our simulations, each iteration consisted of 2×10^4 MC steps (in a MC step all path coordinates and winding number are updated). By using this procedure, the correlator converges after a few iterations. In general, the number of iterations required for convergence increases as the temperature is lowered, but in fact 10 iterations were enough to find convergence in all cases presented here. We have checked that employing different starting correlation functions $G_0(\tau - \tau')$ in our iterative procedure does not change the results.

The conductance $g(T)$ has been obtained from the (self-consistent) correlator G by using the expression¹⁷:

$$g(T) = g_0 \left(\frac{\overline{E}_c}{T} \right)^\epsilon G(\beta/2), \quad (10)$$

where g_0 is the high-temperature conductance.

III. RESULTS

A. Large- N Theory

We now address the self-consistent single grain theory within the large- N approximation, where N is the number of components of the field z_μ . The unimodularity

constraint $\sum_{\mu=1}^N |z_\mu|^2 = 1$ can be imposed with a real Lagrange multiplier field, $\lambda(\tau)$:

$$\mathcal{S} = \int_0^\beta \left\{ \frac{1}{4\overline{E}_c} |\partial_\tau z_\mu|^2 + \lambda(|z_\mu|^2 - 1) \right\} + \tilde{\alpha} \int_0^\beta d\tau \int_0^\beta d\tau' K(\tau - \tau') \{1 - G(\tau - \tau') z_\mu^*(\tau) z_\mu(\tau')\} \quad (11)$$

where $G(\tau - \tau') = \langle z_\mu^*(\tau) z_\mu(\tau') \rangle$ is the self-consistent field due to neighboring sites. The partition function is then obtained by integrating $\exp(-\mathcal{S})$ freely over the complex fields $\{z_\mu(\tau), \bar{z}_\mu(\tau), \lambda(\tau)\}$. In the $N \rightarrow \infty$ limit, the saddle point of the functional integral is dominated by configurations in which $\lambda(\tau)$ is constant. The action, up to a harmless constant, is

$$\mathcal{S} = \sum_{\omega_n} \left(\frac{1}{4} \omega_n^2 + \lambda + \tilde{\alpha} [\hat{Q}(0) - \hat{Q}(\omega_n)] \right) |\hat{z}_\mu(\omega_n)|^2 - \lambda, \quad (12)$$

where we now express all energies in units of E_c . We define $L \equiv \beta E_c$; the bosonic Matsubara frequencies are $\omega_n = 2\pi n/L$. The function $\hat{Q}(\omega_n)$ is the Fourier transform of $Q(s) \equiv K(s)G(s)$, where $s \equiv E_c\tau$ is the dimensionless imaginary time, and

$$K(s) = \left[\frac{\pi}{L} \csc \left(\frac{\pi|s|}{L} \right) \right]^{2-\epsilon}. \quad (13)$$

Thus,

$$\hat{Q}(0) - \hat{Q}(\omega_n) = \int_0^L ds (1 - \cos(\omega_n s)) K(s) G(s). \quad (14)$$

The correlation function $G(s)$ is given by

$$G(s) = \frac{N}{L} \sum_{\omega_n} \frac{e^{i\omega_n s}}{\frac{1}{4}\omega_n^2 + \lambda + \tilde{\alpha}[\hat{Q}(0) - \hat{Q}(\omega_n)]}, \quad (15)$$

and the fixed length constraint is $G(0) = 1$.

We iterate the mean field equations at finite temperature to obtain $\lambda(\tilde{\alpha}, L)$ in the following manner. First, given an initial guess for the set $\{\hat{Q}(\omega_n)\}$, we find λ such that $G(0) = 1$. We then recompute $Q(s) = K(s)G(s)$ and a new set of Fourier components $\{\hat{Q}'(\omega_n)\}$. Iterating until self-consistency, we obtain the results shown in Fig. 1. The self-consistent solutions reveal a discontinuous jump in λ at $\tilde{\alpha}_c$, *i.e.* the transition apparently is first order.

However, it is hardly clear that our iteration scheme should converge to the proper (*i.e.* lowest free energy) self-consistent solution. If the transition is second order, we can make progress by assuming, at criticality ($L = \infty$, $\tilde{\alpha} = \tilde{\alpha}_c$), that

$$G(s) = N \int_0^\infty \frac{d\omega}{\pi} \frac{\cos(\omega s)}{\frac{1}{4}\omega^2 + \tilde{\alpha}_c[\hat{Q}(0) - \hat{Q}(\omega)]}, \quad (16)$$

with $Q(s) = G(s)/|s|^{2-\epsilon}$. Since $G(0) = 1$, we have that $Q(s) \simeq |s|^{\epsilon-2}$ as $s \rightarrow 0$. For s large, we assume $Q(s) \simeq A|s|^{\delta-2}$ and solve for A and δ by ignoring the first term in the denominator of Eq. (16). We find

$$A = \left(\frac{N}{4\pi\alpha_c} (2 - \epsilon) \text{ctn}(\pi\epsilon/4) \right)^{1/2} \quad (17)$$

and $\delta = \frac{1}{2}\epsilon$. Accordingly, we adopt a trial solution for $Q(s)$ which interpolates between the small and large s limits:

$$Q(s) = \frac{e^{-\eta|s|}}{|s|^{2-\epsilon}} + \frac{A(1 - e^{-\eta|s|})}{|s|^{2-\frac{1}{2}\epsilon}}. \quad (18)$$

with η a variational parameter.

Given this trial form for $Q(s)$, we solve $G(0) = 1$ to obtain $\tilde{\alpha}_c(\epsilon, \eta)$. We then check for self-consistency, comparing $G(s)$ obtained from Eq. (16) with $Q(s)|s|^{2-\epsilon}$. We find (i) that $\tilde{\alpha}_c$ is insensitive to η for $\epsilon \lesssim 0.25$, but increasingly sensitive for larger values, and (ii) that there is an optimal value for η , in order that the two definitions of $G(s)$ agree best (see Fig. 2).

Returning to the first order behavior found in the iterated self-consistent solution, we find that this behavior persists for $\epsilon \gtrsim 0.30$. Furthermore, it is hysteretic. The solution shown in Fig. 1 was obtained by sweeping $\tilde{\alpha}$ up from $\tilde{\alpha} = 0$. When a self-consistent solution was obtained, the set $\{\hat{Q}(\omega_n)\}$ was chosen as the initial conditions for iteration for the next value of $\tilde{\alpha}$. When we sweep *both* up and down, however, we find the solution is hysteretic, as shown in Fig. 3. In Fig. 4 we compare $\tilde{\alpha}_c$ obtained assuming a second order transition, as discussed above, with the upper and lower critical values obtained by iteration of the self-consistent equations (with $L = 128$).

B. Monte Carlo simulations

We now turn to the results of our path-integral Monte Carlo simulations for the conductance of the granular system.

In Fig. 5 we present the temperature dependence of the conductance $g(T)$, as derived from our self-consistent correlation function G (squares) for $\tilde{\alpha} = 0.1$ and $\epsilon = 0$, corresponding to a Coulomb-blockade regime. For comparison, we also show MC results found for the same set of parameters for a single junction (circles), for which one finds at low T an algebraic dependence of the conductance in the form $g(T) \sim T^2$, as expected for co-tunneling processes. These processes do not show up in the granular system, and in this case $g(T)$ decreases exponentially as the temperature is lowered.

Our Monte Carlo procedure allows us to study also the dependence of the conductance of the granular system as a function of the offset charge q_i , which appears in the partition function through the phase χ_i . This dependence

is shown in Fig. 6 for the same $\tilde{\alpha}$ value as in Fig. 5 at a temperature $T = E_c/10$. One finds a maximum of the conductance at the degeneracy point ($q_i = 0.5$), similar to the well-known case of a single junction in the presence of Coulomb blockade (solid line in Fig. 6). Again, we observe a decrease in the conductance for the granular system, as compared with the single junction with the same effective parameters $(\tilde{\alpha}, \epsilon)$, in the absence of charge-offset ($q_i = 0$). However, close to the degeneracy point, we find similar values for both systems, that in fact coincide for $q_i = 0.5$ within the error bars of our numerical results.

The conductor-to-insulator phase transition at low temperatures in the parameter space $(\epsilon, \tilde{\alpha})$ can be also analyzed from MC simulations. With this purpose, we have studied the dependence of the conductance on $\tilde{\alpha}$ and T for several values of ϵ . For a given ϵ one expects a conducting regime for $\tilde{\alpha}$ larger than some critical value $\tilde{\alpha}_c$ (see Fig. 4 above). In our numerical analysis this means that we expect a crossover from a region in which g increases (large $\tilde{\alpha}$) to another regime in which g decreases (small $\tilde{\alpha}$) as T is lowered. This is shown in Fig. 7, where we have displayed the dependence of the conductance g on $\tilde{\alpha}$ for $\epsilon = 0.5$ at several temperatures. Each kind of symbols represents MC results at a given temperature, with T increasing from top to bottom in the right part of the Figure. From the crossing point of these curves we can estimate a critical value $\tilde{\alpha}_c = 0.46 \pm 0.02$ for $\epsilon = 0.5$.

In a similar way we have obtained $\tilde{\alpha}_c$ for other ϵ values, and the results are presented in Fig. 8. Symbols are data points derived from MC simulations, and the dashed line is a guide to the eye.

IV. CONCLUSIONS

We have presented a method to analyze the conductance of metallic granular systems in the range of parameters where Coulomb blockade effects are important. The method is a natural extension of the techniques widely used to study the competition between charging effects and tunnel conductance in single junctions. The method allows us to include disorder, and becomes exact when the average coordination number of a grain is large. A related scheme, used to study “grains” with a degenerate level is presented in²⁷. This model is a natural extension of the Hubbard model used to describe the transition between a Mott insulator and a correlated metal, and does show this transition. It would be interesting to compare the properties of this model to the results presented here. A related problem is that of superconducting grains coupled by the Josephson effect. This model, neglecting the effect of normal quasiparticles, has been treated in²⁸, using the CPA method, which is the analog of the Dynamical Mean Field Theory used here.

In the absence of non equilibrium effects, we find that the low temperature behavior of the system is insulating. There is a well defined Coulomb gap at low temperatures,

which, when the intergrain conductances are large, can differ significantly from the intragrain charging energy. This behavior is different from the low temperature conductance of a single junction, where the gapless nature of the leads gives rise to a power law dependence of the conductance, due to cotunneling processes. Our results are valid provided that the temperature is much greater than the intradot level spacing. Within this restriction, and in the absence of non equilibrium effects, we find no evidence for a phase transition between an insulating and a metallic phase²⁹.

Non equilibrium effects can lead to a zero temperature phase transition, in a similar way to the transition which occurs in a single junction. It is interesting to note that this phase transition remains restricted to zero temperature, even when an array of grains with large coordination number is considered. This is so because the most favor-

able case for a metallic regime is when the environment of a given dot is itself metallic. This reduces the problem to that of a single grain connected to metallic leads, which cannot have a finite temperature phase transition, irrespective of the coupling to the leads.

V. ACKNOWLEDGEMENTS.

We have benefited from useful conversations with S. Florens, A. Goerges, G. Kotliar, and A. Zaikin. We acknowledge financial support from CICYT (Spain) through grant PB0875/96, CAM (Madrid) through grant 07N/0045/1998, and the European Union through grant ERBFMRXCT960042.

-
- ¹ I. Giaever and H. R. Zeller, Phys. Rev. Lett. **20**, 1504 (1968).
 - ² J. Lambe and R. C. Jaklevic, Phys. Rev. Lett. **22**, 1371 (1969).
 - ³ P. Sheng, Philos. Mag. B **65**, 357 (1992).
 - ⁴ L. Balcells, J. Fontcuberta, B. Martinez, and X. Obradors, Phys. Rev. B **58**, R14697 (1998).
 - ⁵ J. M. D. Coey, A. E. Berkowitz, Ll. Balcells, F. F. Putris and A. Barry, Phys. Rev. Lett. **80**, 3815 (1998).
 - ⁶ S. Mitani, S. Takahashi, K. Takanashi, K. Yakushiji, S. Maekawa, and H. Fujimori, Phys. Rev. Lett. **81**, 2799 (1998).
 - ⁷ T. Zhu and Y. J. Wang, Phys. Rev. B **60**, 11918 (1999).
 - ⁸ M. García-Hernández, F. Guinea, A. de Andrés, J. L. Martínez, C. Prieto, and L. Vázquez Phys. Rev. B **61**, 9549 (2000).
 - ⁹ F. Fetter, S.-F. Lee, F. Petroff, A. Vaures, P. Holody, L. F. Schelp, and A. Fert, Phys. Rev. B **65**, 174415 (2002).
 - ¹⁰ J. S. Helman and B. Abeles, Phys. Rev. Lett. **37**, 1429 (1976).
 - ¹¹ *Single Charge Tunneling*, H. Grabert and M. H. Devoret eds. (Plenum Press, New York, 1992).
 - ¹² T.-L. Ho, Phys. Rev. Lett. **51**, 2060 (1983).
 - ¹³ E. Ben-Jacob, E. Mottola and G. Schön, Phys. Rev. Lett. **51**, 2064 (1983).
 - ¹⁴ V. Ambegaokar, U. Eckern, and G. Schön, Phys. Rev. Lett. **48**, 1745 (1982).
 - ¹⁵ M. Ueda and S. Kurihara, in *Macroscopic Quantum Phenomena*, edited by T. D. Clark et al. (World Scientific, Singapore, 1990).
 - ¹⁶ M. Ueda and F. Guinea, Zeits. für Phys. B **85**, 413 (1991).
 - ¹⁷ E. Bascones, C. P. Herrero, F. Guinea, and G. Schön, Phys. Rev. B **61**, 16778 (2000).
 - ¹⁸ Ya. M. Blanter, A. D. Mirlin and B. A. Muzykantskii, Phys. Rev. Lett. **78**, 2449 (1997).
 - ¹⁹ A. Georges, G. Kotliar, W. Krauth, and M. J. Rozenberg, Rev. Mod. Phys. **68**, 13 (1996).
 - ²⁰ S. Renn, cond-mat/9708194.
 - ²¹ D. Arovas, and S. Drewes, to be published.
 - ²² C. P. Herrero, G. Schön, and A. D. Zaikin, Phys. Rev. B **59**, 5728 (1999).
 - ²³ G. Schön and A. D. Zaikin, Phys. Rep. **198**, 238 (1990).
 - ²⁴ G. D. Mahan, *Many-Particle Physics* (Plenum, New York, 1991).
 - ²⁵ C. Kane and M. P. A. Fisher, Phys. Rev. B **46**, 15233 (1992).
 - ²⁶ *Quantum Monte Carlo Methods in Condensed Matter Physics*, edited by M. Suzuki (World Scientific, Singapore, 1993).
 - ²⁷ S. Florens, and A. Georges, Phys. Rev. B **66**, 165111 (2002).
 - ²⁸ W. A. Al-Saidi, and D. Stroud, cond-mat/0211539.
 - ²⁹ K. B. Efetov, and A. Tschersich, Europhys. Lett. **59**, 114 (2002). Note that the methods used in this reference cannot be applied to scales of order $E_c e^{-\tilde{\alpha}}$, using our notation.

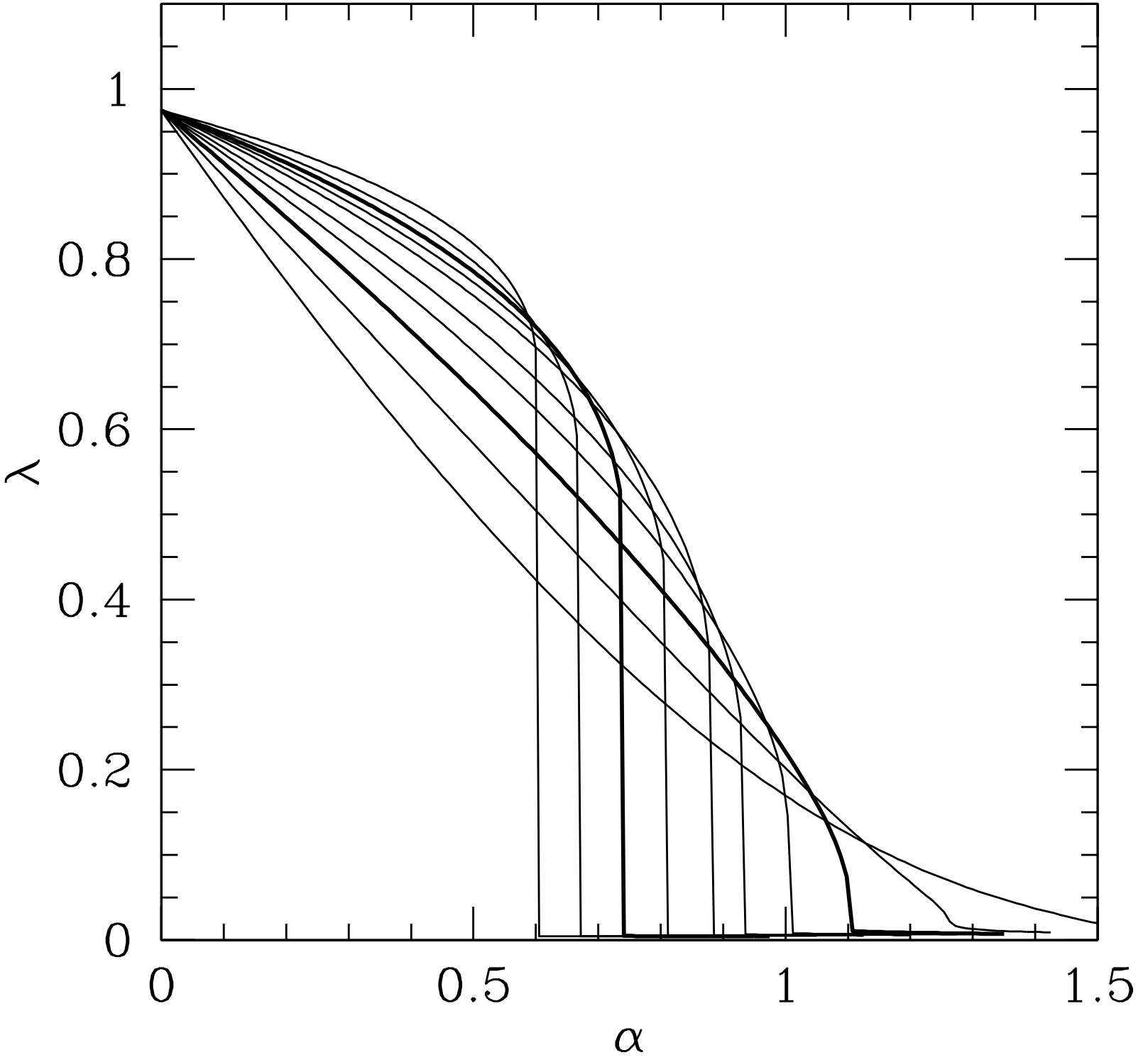


FIG. 1: Solution to the large- N theory for $L = 128$ and $\epsilon = 0.1, 0.3, 0.5, \dots, 1.9$. $\tilde{\alpha}_c$ decreases with increasing ϵ . Thick curves are for $\epsilon = 0.5$ and $\epsilon = 1.5$.

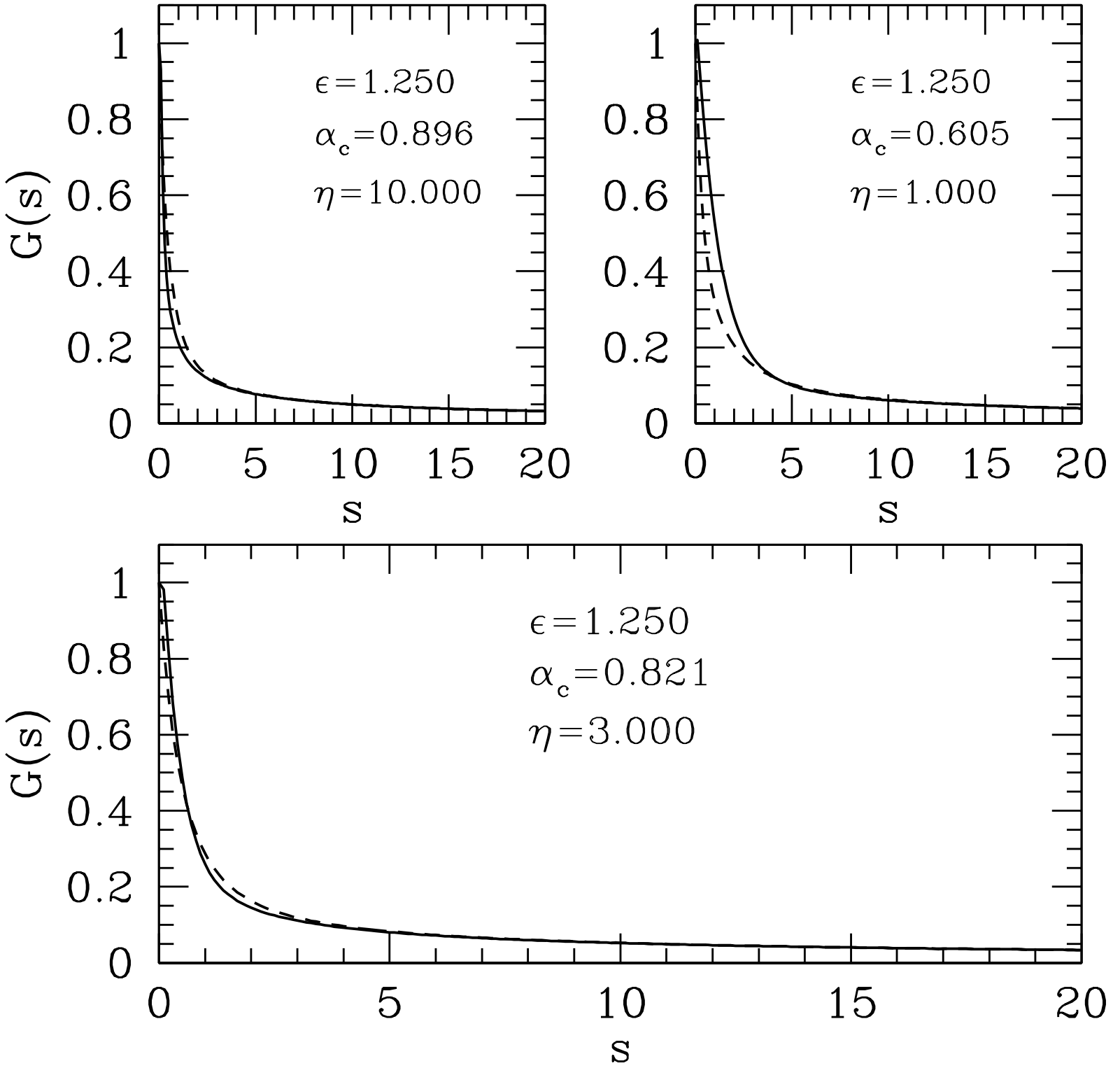


FIG. 2: Correlation function $G(s)$ at criticality *versus* dimensionless imaginary time s . Solid line is input $G(s) = e^{-\eta|s|} + A(1 - e^{-\eta|s|})|s|^{-\frac{1}{2}\epsilon}$; dashed line is obtained from Eq. 16. Here $\eta = 3.00$ provides the best fit of the three curves.

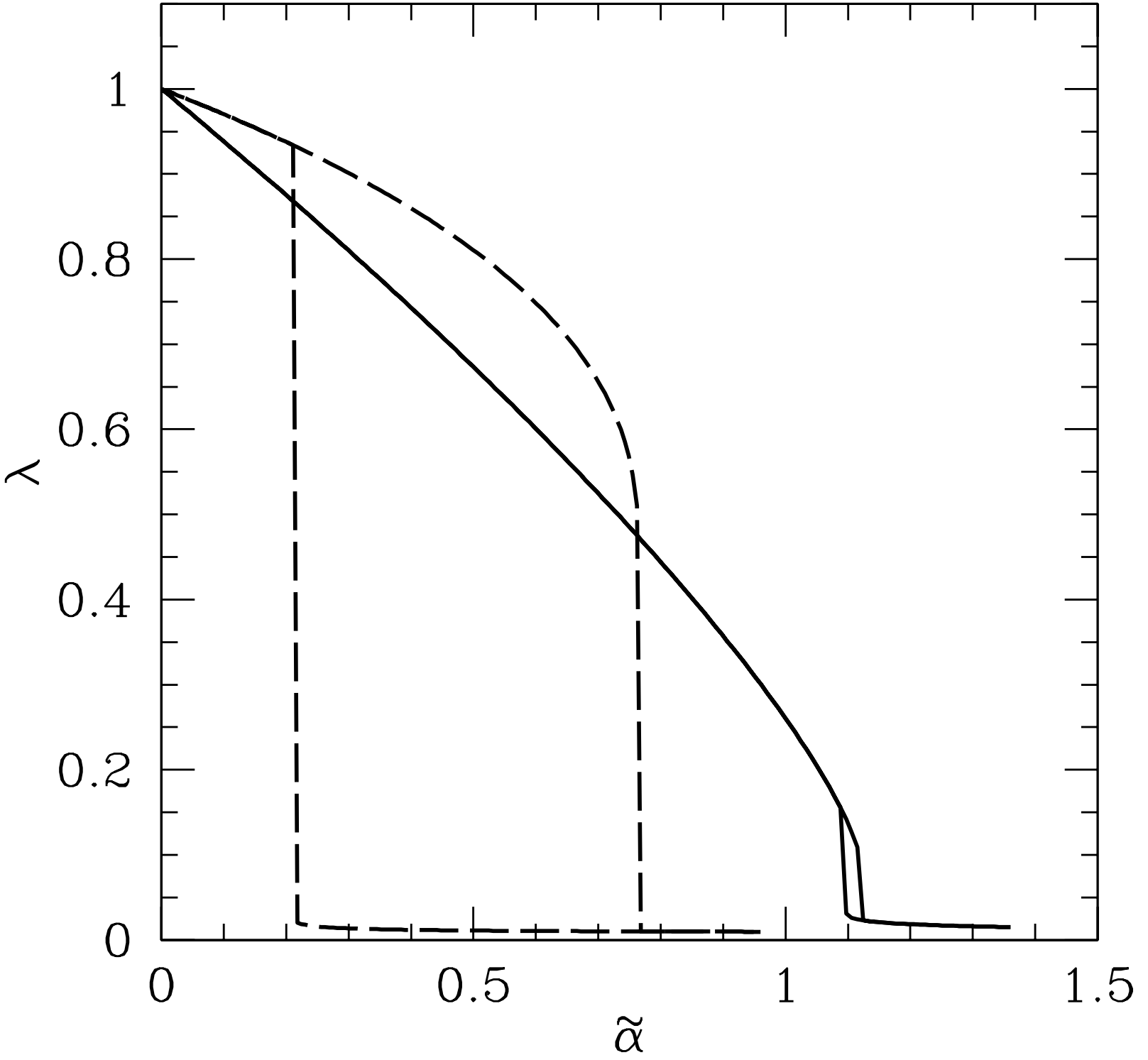


FIG. 3: Hysteretic behavior in the self-consistent solution for $L = 128$. Solid curves are for $\epsilon = 0.50$; dashed curves are for $\epsilon = 1.50$.

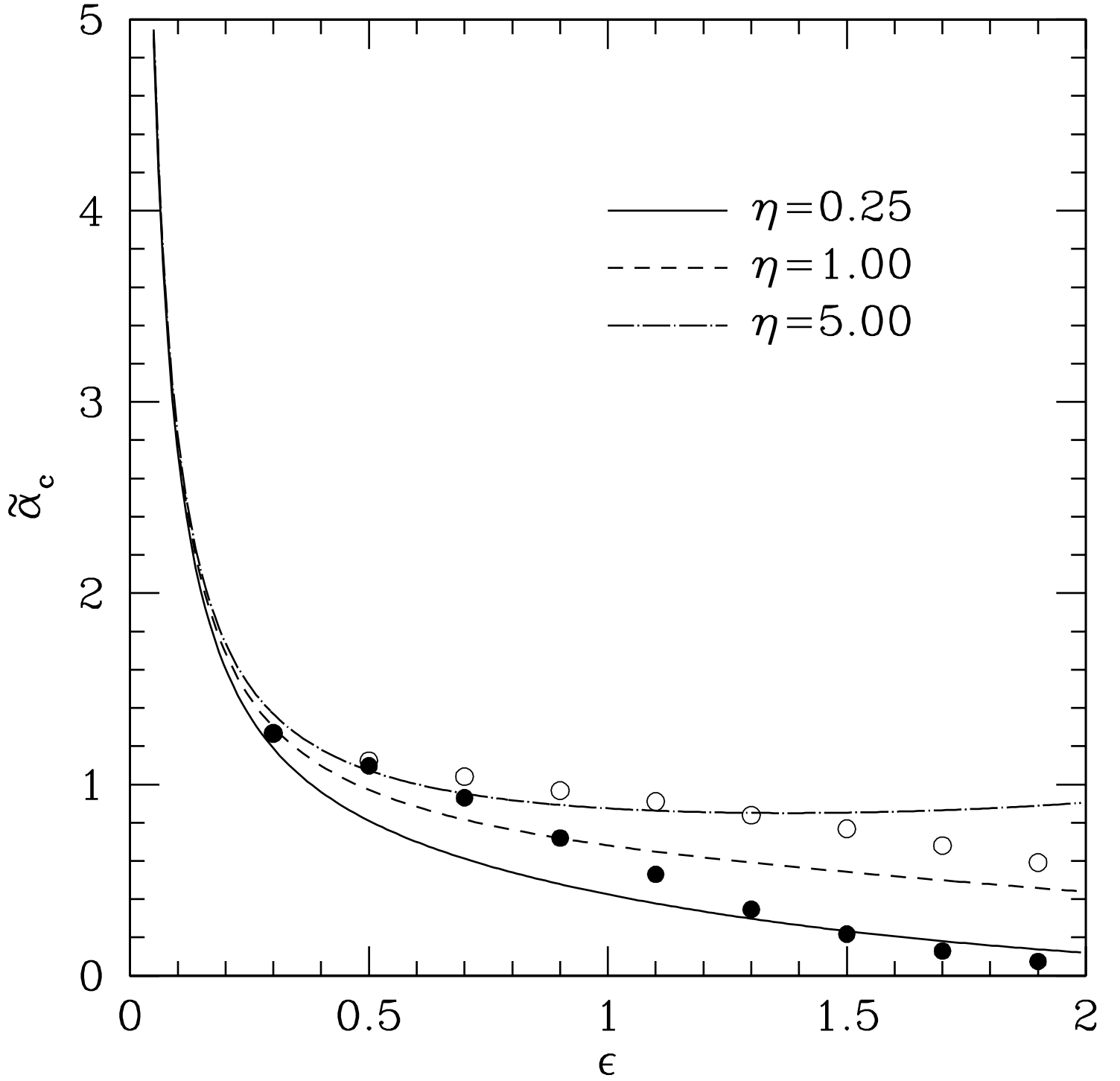


FIG. 4: $\tilde{\alpha}_c$ versus ϵ for three different values of η (curves). Open and closed circles denote maximum and minimum values of $\tilde{\alpha}_c$ inferred from iterative solution to the self-consistent equations with $L = 128$.

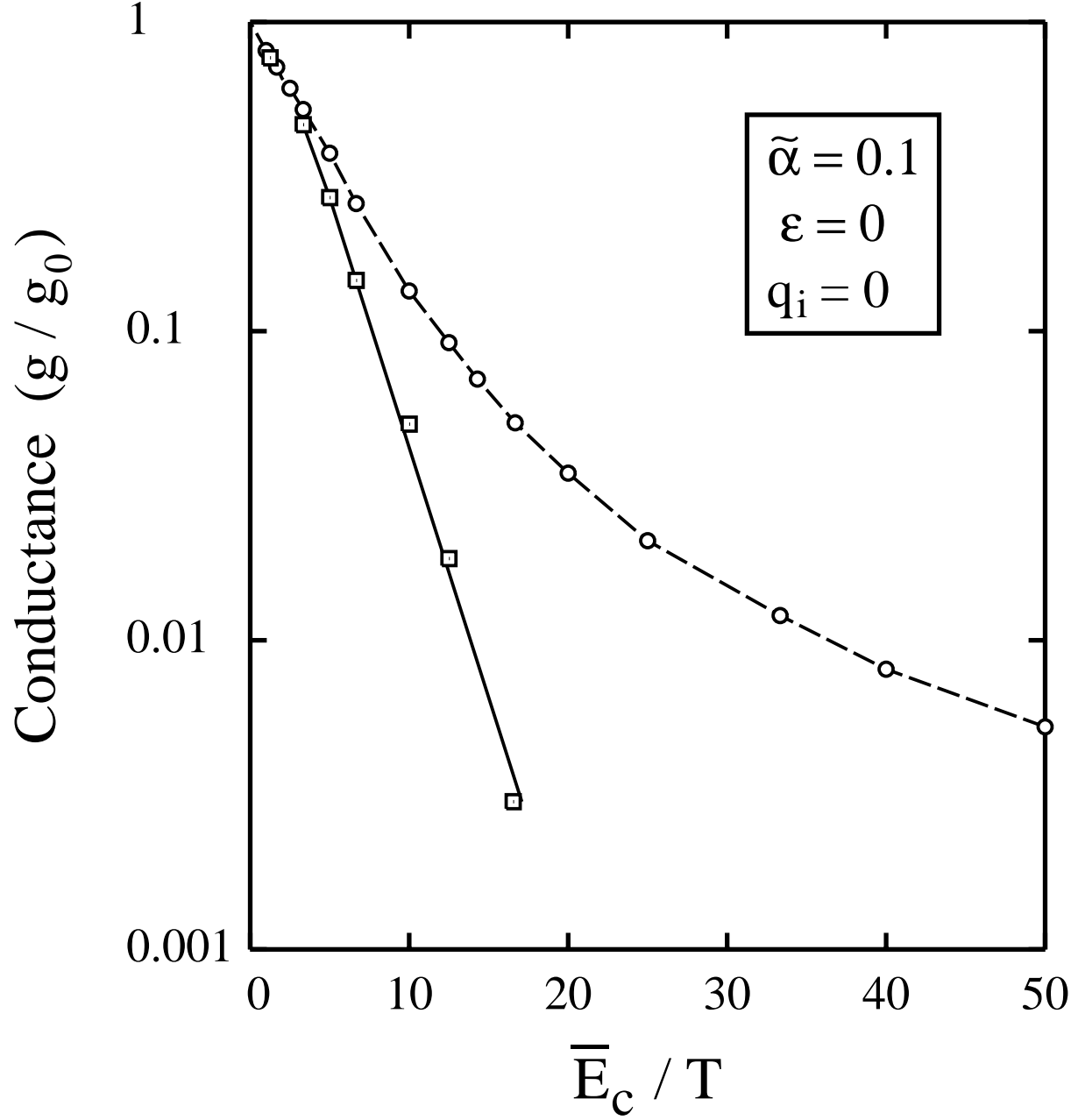


FIG. 5: Temperature dependence of the normalized conductance g/g_0 , as derived from path-integral Monte Carlo simulations for a granular system (squares) and for a single tunnel junction (circles) with the same parameters: $\tilde{\alpha} = 0.1$, $\epsilon = 0$, and $q_i = 0$ (no offset charge). Error bars are on the order of the symbol size.

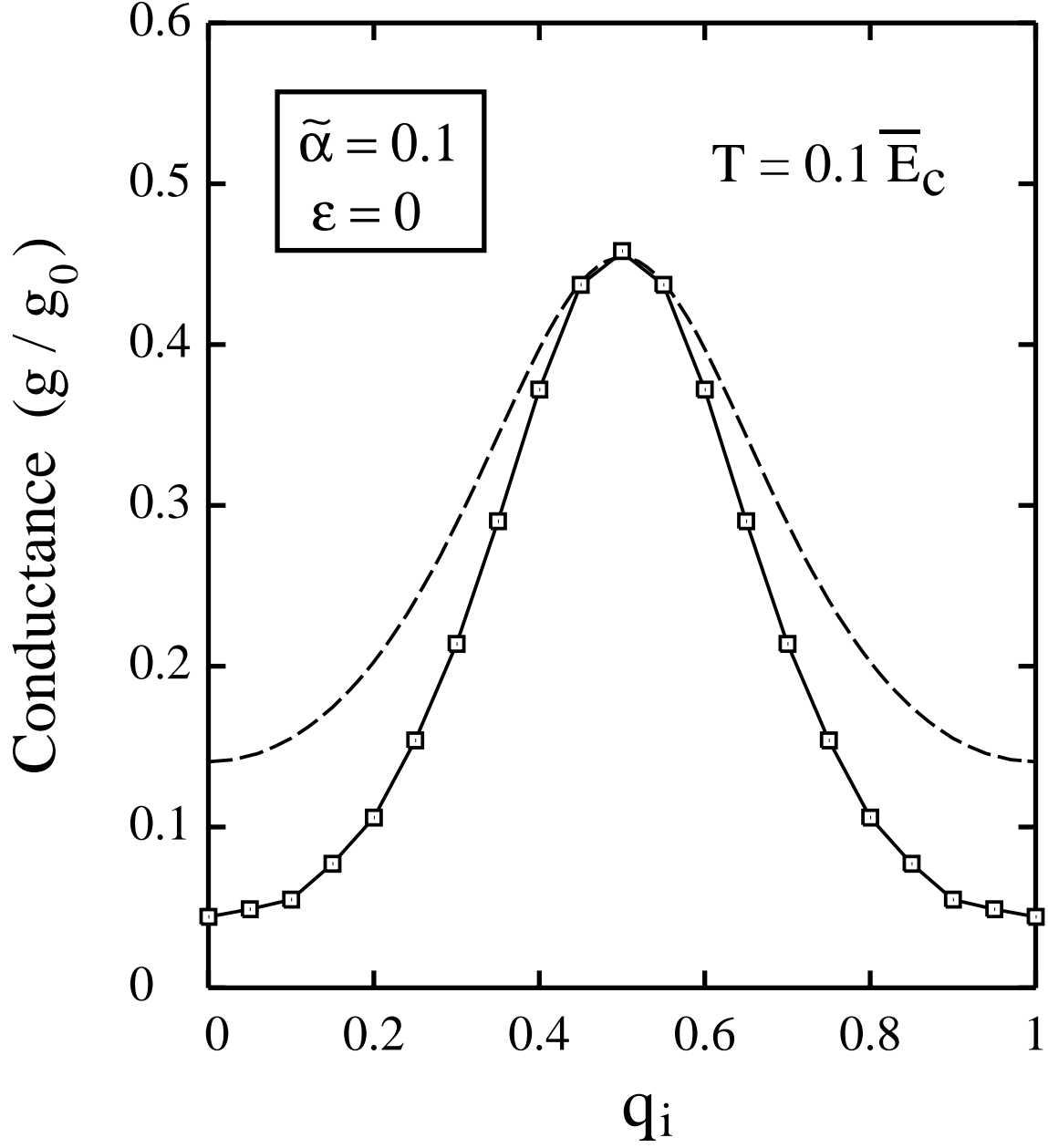


FIG. 6: Normalized conductance (g/g_0) vs. offset charge q_i , as derived from Monte Carlo simulations for a granular system (squares) and for a single tunnel junction (dashed line) with the same parameters: $\tilde{\alpha} = 0.1$, $\epsilon = 0$, and $T = \bar{E}_c/10$.

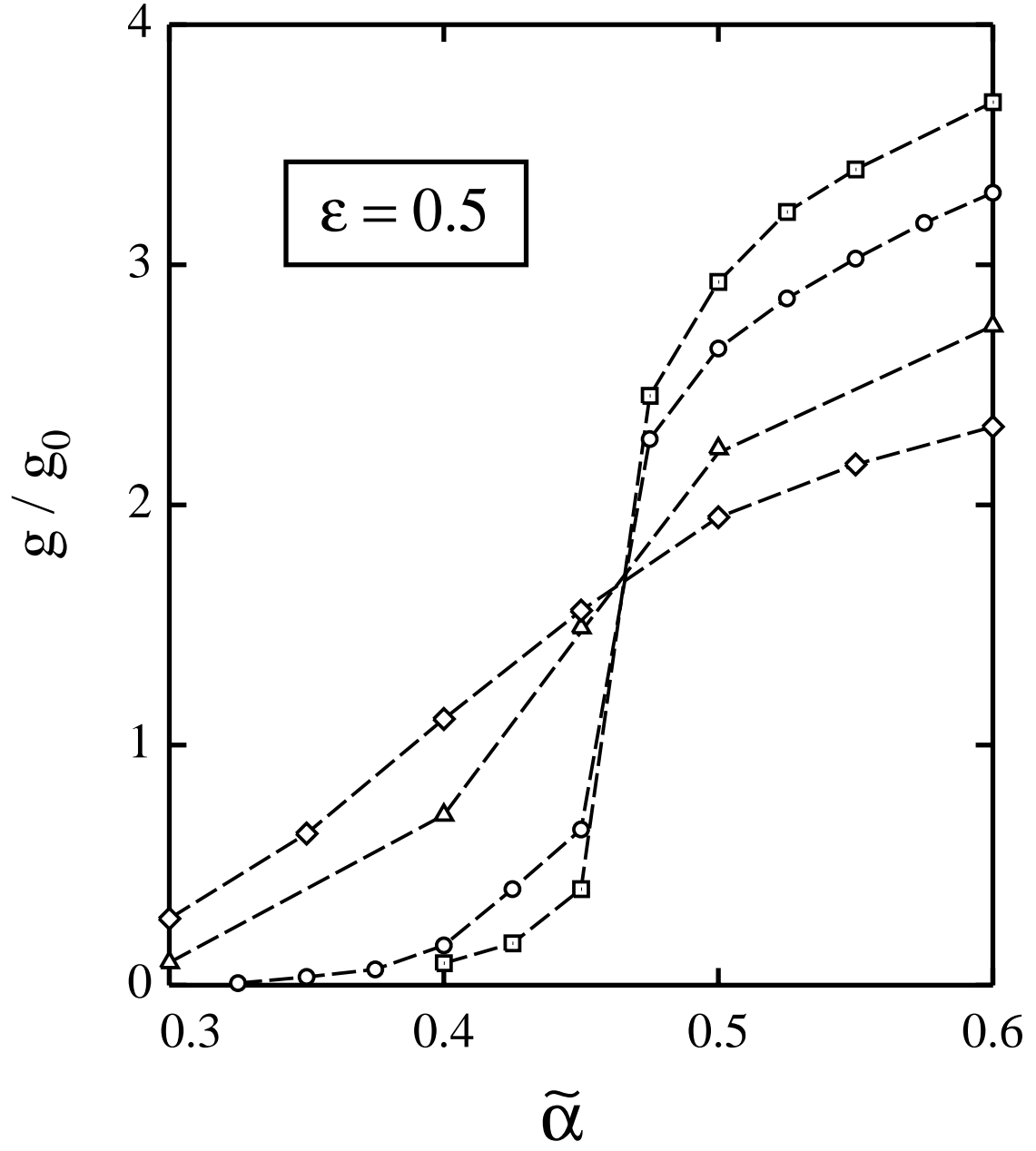


FIG. 7: Normalized conductance as a function of $\tilde{\alpha}$ for a granular system with $\epsilon = 0.5$. Different symbols represent several temperatures: $\beta E_c = 40$ (squares), 30 (circles), 20 (triangles), and 14 (diamonds).

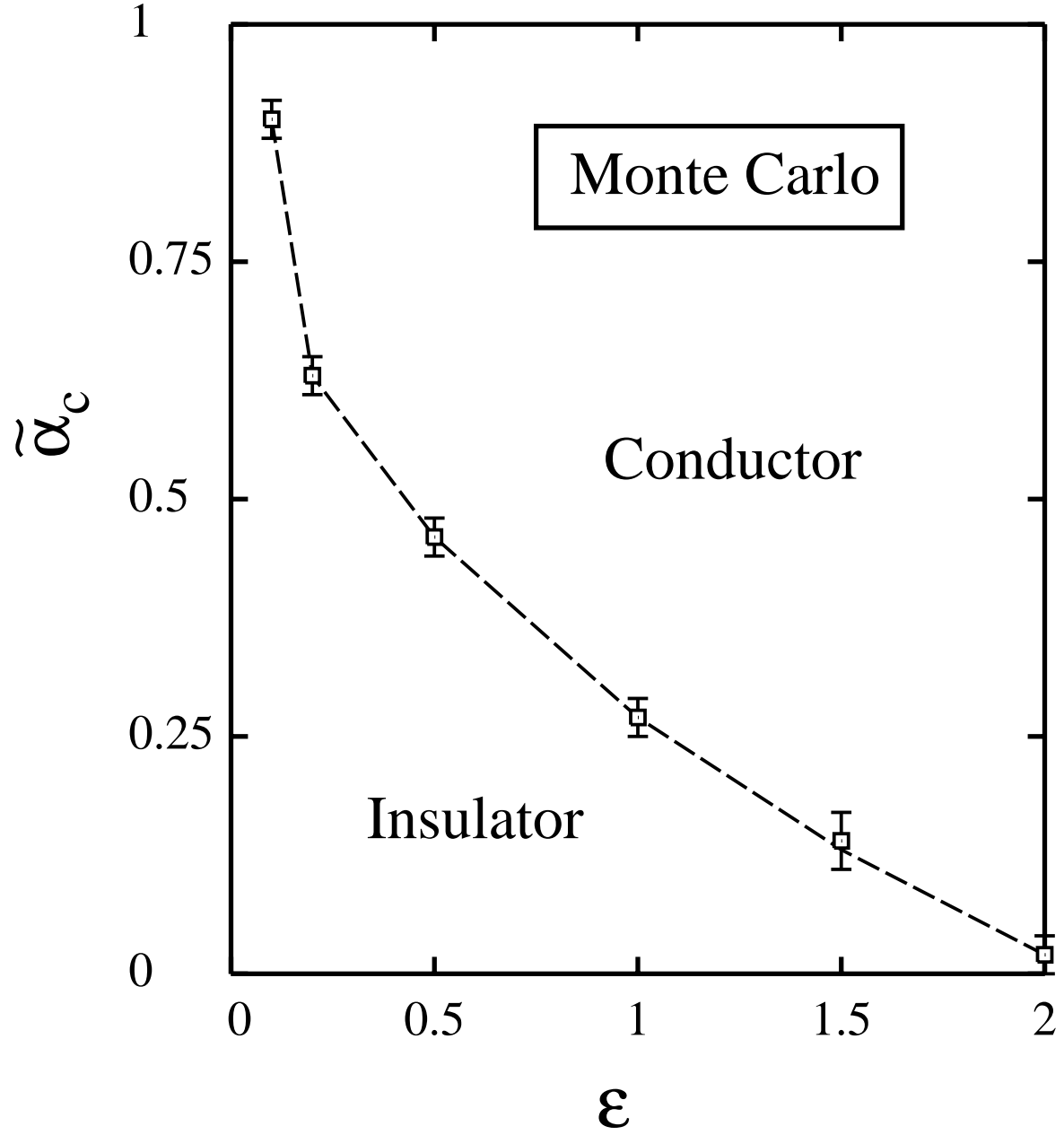


FIG. 8: The critical value of the parameter $\tilde{\alpha}$ for the insulator-to-conductor transition is plotted vs the parameter ϵ . Symbols were derived from Monte Carlo simulations, as indicated in the text.